Hindawi
International Journal of Energy Research
Volume 2023, Article ID 3415211, 8 pages
https://doi.org/10.1155/2023/3415211

WILEY | Hindawi

Research Article

High-Output Wearable Flow Ring-Based Triboelectric Nanogenerator via Opposite Charging Intermediate Layer

Seh-Hoon Chung,[1] Yu Ha Jang,[1] Dongchang Kim,[1] Joon-seok Lee,[1] Sunghan Kim,[1] Joong Yull Park,[1] Jinkee Hong,[2] and Sangmin Lee[1]

[1]*School of Mechanical Engineering, Chung-Ang University, 84 Heukseuk-ro, Dongjack-gu, Seoul 06974, Republic of Korea*
[2]*School of Chemical & Biomolecular Engineering, Yonsei University, 50 Yonsei-ro, Seodaemun-gu, Seoul 03722, Republic of Korea*

Correspondence should be addressed to Jinkee Hong; jinkee.hong@yonsei.ac.kr and Sangmin Lee; slee98@cau.ac.kr

Received 8 November 2022; Revised 17 December 2022; Accepted 19 December 2022; Published 13 February 2023

Academic Editor: Samarjeet Singh Siwal

Triboelectric nanogenerator (TENG) is one of the emerging energy harvesting technologies with the potential to be an alternative energy source. Owing to the various advantages of TENG, such as low cost, simple design, and high applicability, several researchers reported wearable TENG devices that can power electronics by harvesting human motion. However, as the human body has limited movement, the existing wearable TENG devices can only generate low power to turn on the electronics. In this study, a flow ring-based TENG (FR-TENG) is fabricated, which can be applied to wearable devices to generate high voltage and current output by including an opposite charging intermediate layer. By the simulation and experimental results, FR-TENG is optimized to generate a high output, that is, peak open-circuit voltage and closed-circuit current of up to 1020 V and 260 mA, respectively, owing to the electrostatic discharge. By these results, sleeve-type wearable FR-TENG is fabricated which can effectively harvest energy from arm movement. The sleeve-type FR-TENG can generate a high output owing to the working mechanism of FR-TENG; the high output was used to turn on 200 LEDs.

1. Introduction

Triboelectric nanogenerator (TENG) is one of the emerging energy harvesting technologies that can convert discarded mechanical energy such as human movement [1–3], wind [4–6], and wave power [7–9] into electrical energy. TENG has the potential to be an alternative energy source with various advantages such as low cost, simple design, and high applicability. Owing to its advantages, various studies have been reported on the practical applications of TENG [10–12]. Notably, several researchers reported wearable TENG devices that can power electronics by human movement [13–15]. Owing to the high applicability of TENG, various wearable TENGs have been demonstrated, which can be utilized for different body parts such as the arm [16], leg [17], and skin [18, 19]. Accordingly, wearable TENG can harvest wasted mechanical energy from various human movements such as exercising [20]. However, existing wearable TENG can only generate low electrical output due to the fundamental mechanism of TENGs and limited input energy. Generally, TENG can only generate few microamperes of current output. Even though, several studies have reported that fabricating nano-micro-surfaces [21], utilizing external circuits such as charge pump circuit and charge excitation circuit [22], and using novel materials [23] can increase current output of TENG; most of these methods are hard to be utilized for wearable TENGs by the complex structure. Moreover, as the human body has limited movement, the wearable TENG can only harvest energy from limited mechanical input. In addition, as the size of wearable TENG has to be adjusted to the human body, the size of wearable TENG is limited. As the TENG can generate electricity by the surface charge of dielectric surface, small size of the device results in low power [24]. As a result, wearable TENGs generate

low output, which is a critical limitation for powering electronics applications. Therefore, it is necessary to develop a new TENG mechanism that can generate a high output even with limited movement by compact structure to fabricate practical wearable TENG.

In this study, we demonstrate flow ring-based TENG (FR-TENG) that can generate high output with limited movement by including an opposite charging intermediate layer. FR-TENG consists of a flow ring, which is used as a conductor, charging layer, and electric circuit. When the flow ring passes through the charging layer, the charges inside the flow ring are polarized. The polarized charges result in an electric potential difference between the flow ring and the electrode circuit, thus generating an electrostatic discharge. Moreover, FR-TENG includes an opposite charging intermediate layer, which can enhance the electric potential difference. Thus, FR-TENG can generate a high electrical output based on robust electrostatic discharge. Moreover, by optimizing with the simulation and experimental results, FR-TENG can generate a high peak electrical output of up to 1020 V and 260 mA, respectively. As FR-TENG can generate a high output with limited movement, wearable sleeve-type FR-TENG is fabricated for practical applications. Even with limited human arm movement, sleeve-type FR-TENG can generate peak voltage and current output of up to 620 V and 166.4 mA, respectively. Consequently, sleeve-type FR-TENG with a rectifying circuit can turn on 200 light-emitting diodes (LEDs), which demonstrates that FR-TENG can be used as a power source for electronic devices.

2. Materials and Methods

2.1. Fabrication of FR-TENGs. FR-TENG consists of a flow ring (Toroflux), polymethylmethacrylate (PMMA) rod (diameter: 5 cm and length: 90 cm), PTFE tape, nylon sheet, and aluminum tape with a thickness of 0.05 mm (Ducksung Hitech Co.). The PMMA rod is covered by PTFE tape, and the nylon sheet and aluminum tape are attached to the PTFE tape. Nylon sheets are attached with a point 16 cm from the center of the PMMA rod covered with PTFE tape as the center point of the sheet.

In addition, sleeve-type FR-TENG is constructed based on a commercial nylon sleeve (PS2000, 3M Co.). The 4 cm $\times$ 4 cm PTFE film and 2 cm $\times$ 2 cm aluminum tape are attached to the commercial nylon sleeve, and the aluminum tape is connected by an electric wire. In addition, ultrafast switching diodes (MUR460, Motorola Co.) are used for rectifying circuit for FR-TENG. Also, commercial green LEDs (5BG4UC00, Dakwang Co.) are used for the application.

2.2. Finite Element Simulation. The simulation result of FR-TENG is obtained by using finite element simulation program of COMSOL Multiphysics (COMSOL Co.). To verify the effect of opposite charging intermediate layer, the electrical field strength with and without opposite charging intermediate layer is shown in the simulation result. The surface charge density of the nylon film and PTFE film is set as 2.83 μC/m^2 and -10.8 μC/m^2, respectively. The relative permittivity of air, Al electrode, PTFE, and nylon is set as 1, 1, 2.1, and 4, respectively. In addition, floating potential is given in every boundary of Al electrode.

2.3. Electrical Measurements. Voltage and current outputs were measured using an oscilloscope (MDO 3014, Tektronix Co.) with differential (THDP0100, Tektronix Co.) and current probes (TCP0030A, Tektronix Co.).

3. Results and Discussion

Flow ring-based triboelectric nanogenerator (FR-TENG) consists of four parts: stainless steel flow ring, polytetrafluoroethylene (PTFE) rod, nylon film, and electrodes (Figure 1(a)). The nylon films are attached to the PTFE rod, and the electrodes are attached to each nylon film. As shown in Figure 1(b), the flow ring can pass through the PTFE rod. When the flow ring comes in contact with the attached electrodes, FR-TENG can generate an electrical output owing to triboelectricity. As the PTFE surface contains negative charges, the negative charges separate the charges inside the flow ring. When the flow ring comes in contact with the attached electrodes, the negative charges in the flow ring are released to the attached electrodes, and an output is generated. As the FR-TENG is operated by the movement of the flow ring, it can be utilized as a wearable energy harvesting device for harvesting the mechanical energy of human movement, as shown in Figure 1(c). As the flow ring can slide over the human arm, the charges on the commercial sleeve can also generate charges in the flow ring. This effect enables the fabrication of wearable FR-TENG that can generate electricity with human movement.

A high voltage output can be generated in FR-TENG by inserting the opposite charging layer, such as a nylon film, between the electrode and the PTFE rod. Owing to the positive charges on the nylon film, the positive and negative charges are separated in the attached electrodes. Thus, the positive charges in the attached electrodes lead to a high potential difference between the flow ring and attached electrodes, which results in an electrostatic discharge. Thus, by this mechanism, FR-TENG can generate a high output. The detailed working mechanism of FR-TENG is explained in a later paragraph. Figure 1(d) shows the finite element simulation result of the electrical field of FR-TENG with and without the nylon layer as the opposite charging intermediate layer using COMSOL. The surface charge density of the nylon film and PTFE film is set as 2.83 μC/m^2 and -10.8 μC/m^2, respectively [25]. According to the simulation result, a higher electric field is generated when the nylon film is used. Owing to the high potential difference, the high peak open-circuit voltage (V_{OC}) and closed-circuit current (I_{CC}) outputs of FR-TENG are 676 V and 204 mA, respectively (Figures 1(e) and 1(f)).

Figure 2(a) shows the detailed working mechanism of the FR-TENG. Figure 2(a), i shows the schematic of FR-TENG without the nylon intermediate layer, and Figure 2(a), ii shows the schematic of FR-TENG with the nylon intermediate layer. When the flow ring slides along the PTFE-based substrate, the negative charges of the PTFE surface separate the charges inside the flow ring. As a result, positive charges

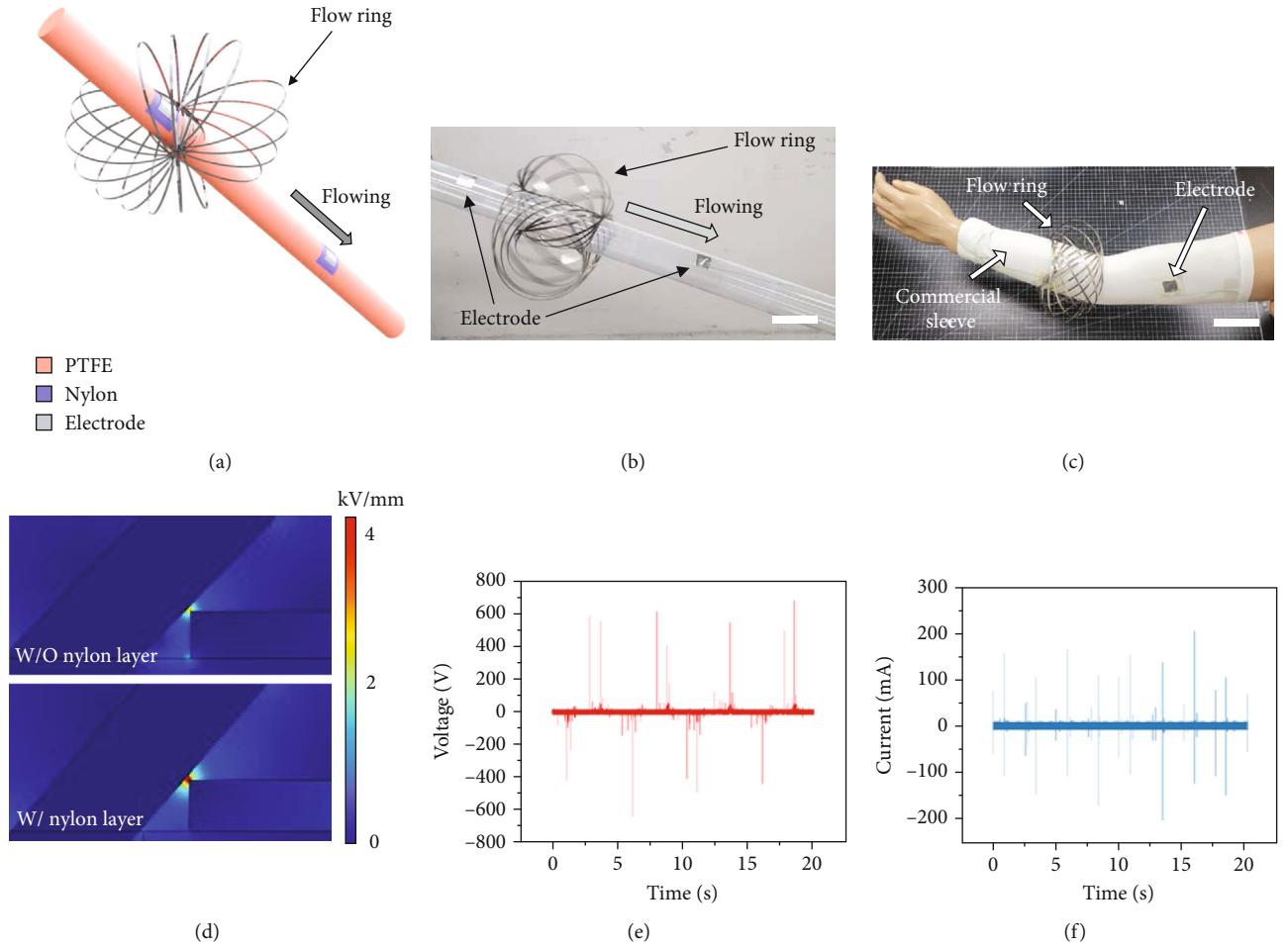

Figure 1: Flow ring-based triboelectric nanogenerator (FR-TENG). (a) Schematic illustration of FR-TENG. Photograph of working (b) FR-TENG and (c) sleeve-type FR-TENG (scale bar: 10 cm). (d) Simulation result of FR-TENG with nylon layer and without nylon layer. (e) V_{OC} and (f) I_{CC} outputs of FR-TENG.

are located close to the PTFE-based substrate, and negative charges are located far from the PTFE-based substrate, as shown in Figure 2(a), i. When the flow ring comes in contact with the attached electrode, the negative charges inside the flow ring are released to the attached electrode, and electrical output is generated. The electrical output can be enhanced by adding the opposite charging intermediate layer. As shown in Figure 2(a), i, the charges in the attached electrode can be polarized by the surface charge of the PTFE-based substrate [26]. Owing to the negative charges of the PTFE surface, the charges inside the electrode are polarized. As the positive charges are located near the PTFE surface, the negative charges are located at the exterior of the electrode. Owing to these negative charges, a low potential difference is generated between the flow ring and the electrode. However, when the nylon intermediate layer is attached between the PTFE and the electrode, the charges are oppositely polarized in the electrode. As shown in Figure 2(a), ii, the negative charges are induced by the positive charge of the nylon layer. Owing to this effect, the positive charges are located at the exterior of the electrode. The positive charges result in a high potential difference between the flow ring and the electrode. In this way, the electrical output of FR-TENG can be increased. Figures 2(b) and 2(c) show the measured V_{OC} and I_{CC} of FR-TENG with and without the nylon layer. As shown in Figure 2(b), the peak V_{OC} of FR-TENG without and with the nylon layer is 575 V and 1020 V, respectively. In addition, the peak I_{CC} of FR-TENG without and with the nylon layer is 139.2 mA and 260 mA, respectively. Consequently, the measured result indicates that the nylon layer can enhance the electrical output of FR-TENG.

Similar to the mechanism explained in the previous paragraph, the electrical output in the case of the nylon-based substrate can be also enhanced by including a PTFE layer. As shown in Supplementary Information 1, when the FR-TENG is constructed using a nylon-based substrate, the positive charges of the nylon surface induce the negative charges in the flow ring. As a result, the positive charges are polarized in the flow ring. The induced positive charges result in a potential difference between the ring and electrodes. Through this effect, FR-TENG can generate electricity with the nylon-based substrate. Similar to the PTFE-based FR-TENG, the electrical output of nylon-based FR-TENG can be enhanced. Owing to the negative charge of the PTFE

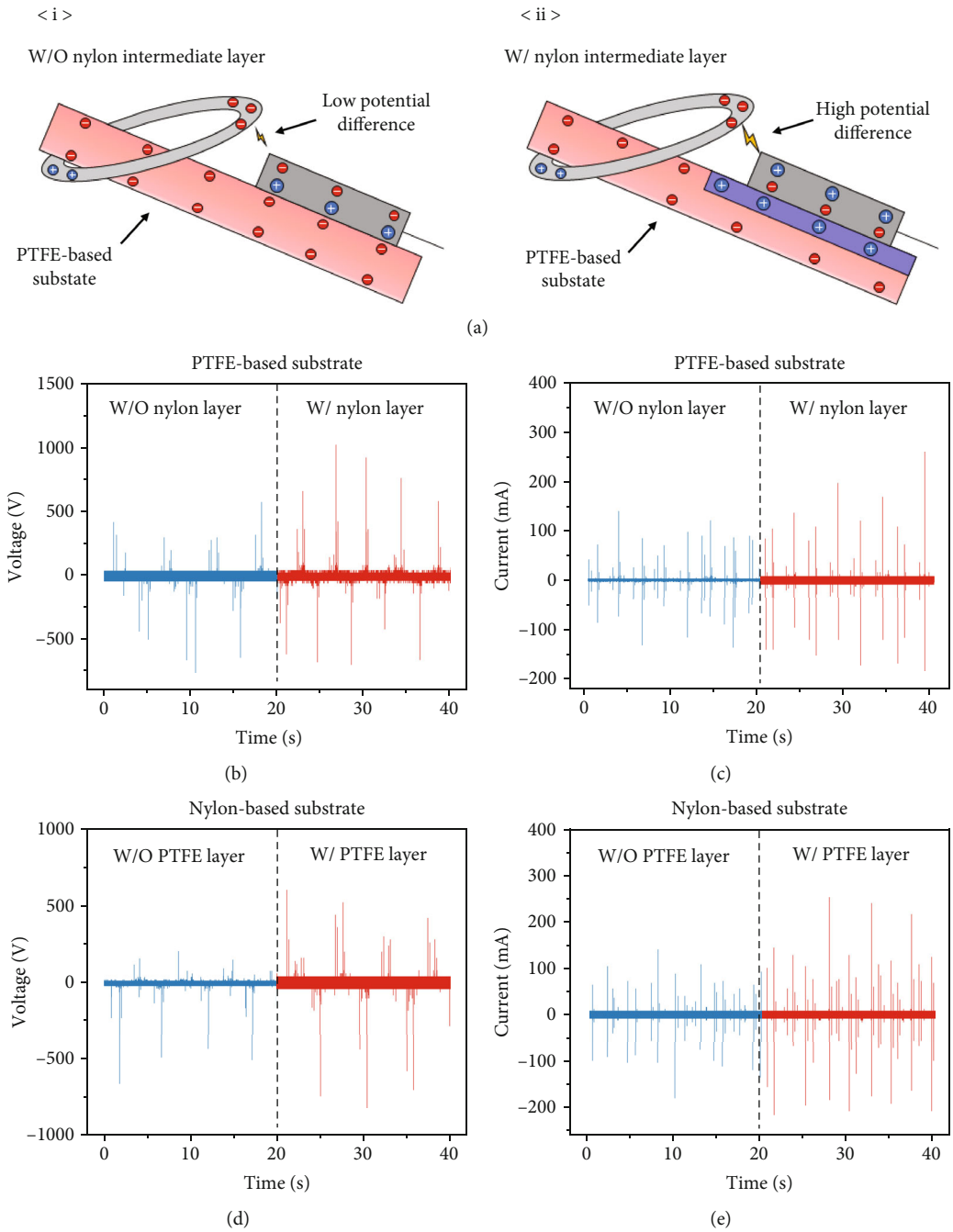

Figure 2: Working mechanism and output of the FR-TENG. (a) Schematic of the FR-TENG without nylon layer and with nylon layer. (b) V_{OC} and (c) I_{CC} outputs of PTFE-based FR-TENG without nylon layer and with nylon layer. (d) V_{OC} and (e) I_{CC} outputs of nylon-based FR-TENG without PTFE layer and with PTFE layer.

layer, charges are polarized in the attached electrode. As the negative charges are located at the exterior of the attached electrode, a high potential difference is generated between the flow ring and the attached electrode. Through this effect, the electrical output of nylon-based substrate can be enhanced. In Supplementary Information 2, the simulation result shows that the electrical field intensity between the flow ring and the attached electrode increased with the use of the PTFE layer. For the nylon-based FR-TENG without the PTFE layer, the electric field intensity goes up to 0.8 kV/mm. However, when the nylon-based FR-TENG contains a PTFE layer, the electric field intensity increases to 7.33 kV/mm. This simulation result indicates that including a PTFE layer for nylon-based FR-TENG can enhance the electrical output. Accordingly, the peak V_{OC} and I_{CC} were increased by adding a PTFE layer as the opposite charging intermediate layer, as shown in Figures 2(d) and 2(e). When the nylon-based substrate is used for FR-TENG, the V_{OC}

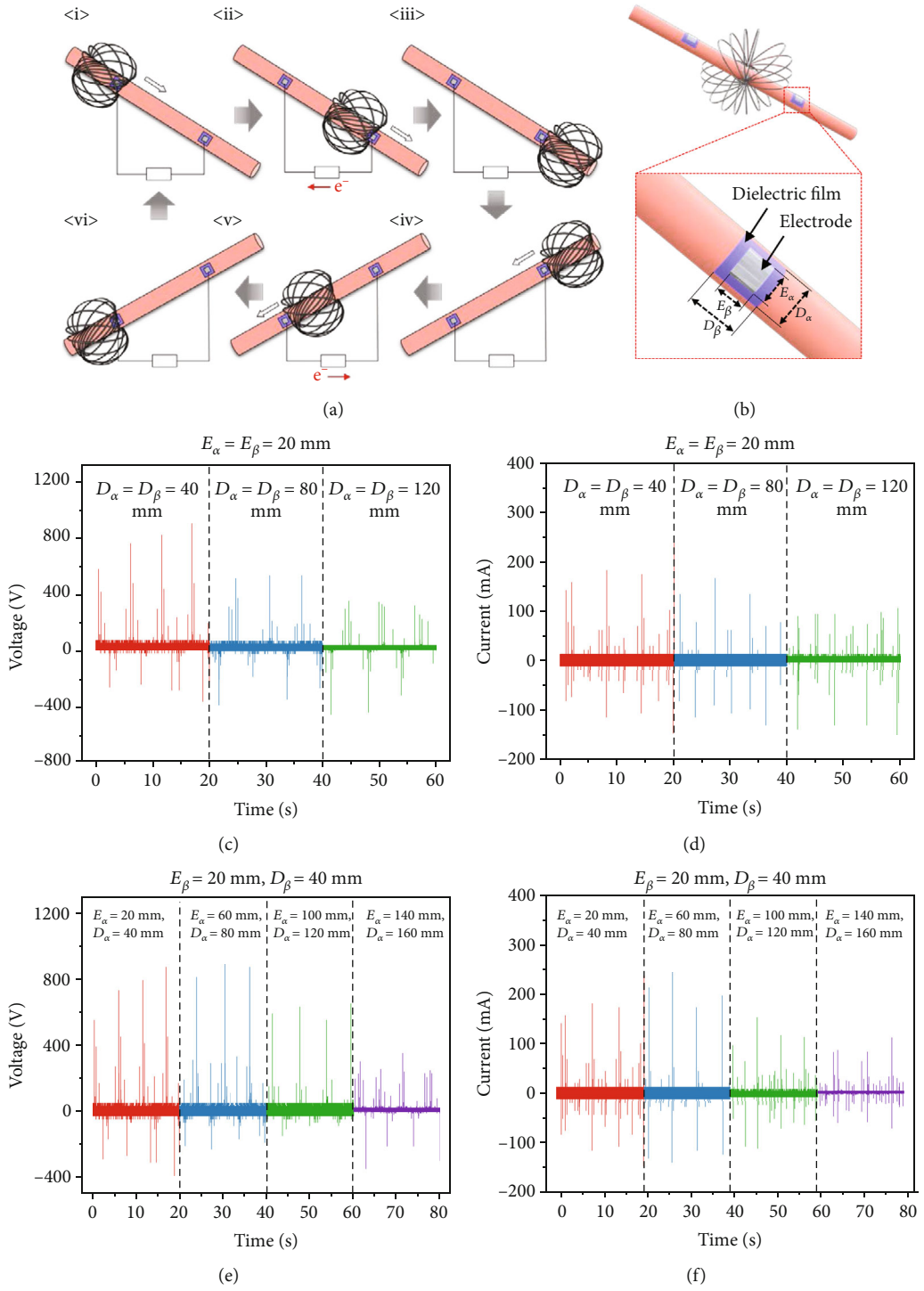

FIGURE 3: Parametric study of FR-TENG. (a) Schematic of the working mechanism of FR-TENG. (b) Cross section of FR-TENG. (c) V_{OC} and (d) I_{CC} outputs of FR-TENG with different areas of the dielectric film. (e) V_{OC} and (f) I_{CC} outputs of FR-TENG with different horizontal lengths.

output of FR-TENG with and without the PTFE layer is 204 V and 600 V, respectively. In addition, the I_{CC} output of FR-TENG with and without the PTFE layer is measured up to 140 mA and 252 mA, respectively. As a result, the electrical output can be increased by utilizing an oppositely charged material layer, such as a nylon layer for PTFE-based FR-TENG and PTFE layer for nylon-based FR-TENG.

The movement of the flow ring is described in Figure 3(a). Because of the slope of the FR-TENG, the flow ring passes through the PTFE rod. Owing to the surface charge of the

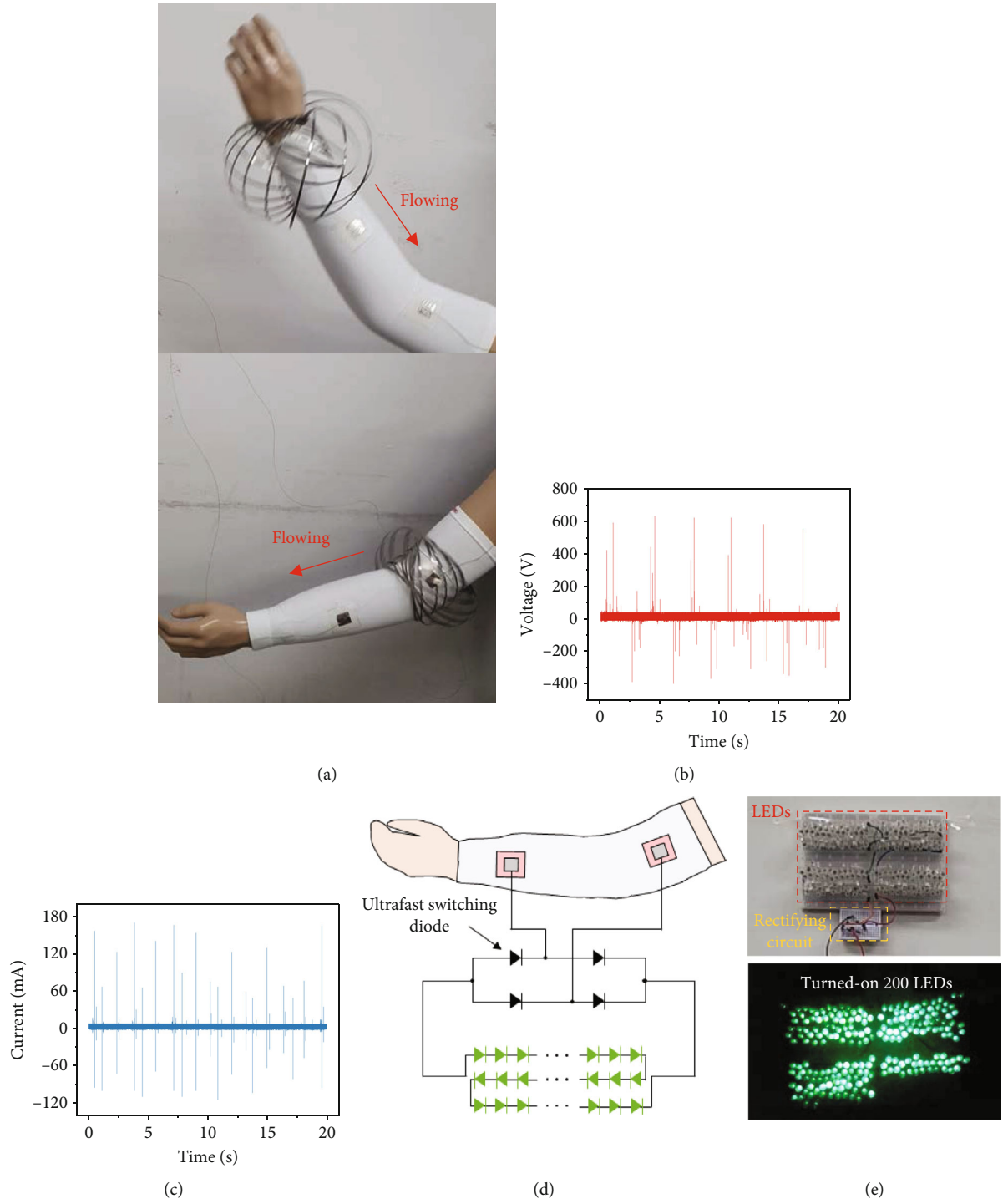

Figure 4: Application of the FR-TENG. (a) Photographs of working sleeve-type FR-TENG. (b) V_{OC} and (c) I_{CC} outputs of sleeve-type FR-TENG. (d) Schematic of rectifying circuit for sleeve-type FR-TENG and (e) the photographs of the circuit and 200 LEDs turned on by the movement of sleeve-type FR-TENG.

PTFE rod, the charges are induced in the flow ring. When the flow ring comes in contact with the electrode, as described in Figure 3(a), ii, the induced negative charges are released to the electrode and generate electrical output. When the slope of the FR-TENG is in the opposite direction, the flow ring slides again. By the same mechanism, charges are accumulated in the flow ring and released when the flow ring comes in contact with the electrode. For a better understanding of the mechanism and optimization of FR-TENG, several parametric studies are shown in Figures 3(b)–3(f). Figure 3(b) shows the length variables of the attached films of FR-TENG that can be optimized. E_α and E_β are the longitudinal

length and tangential length of the electrode, respectively. D_α and D_β are the longitudinal and tangential lengths of the dielectric film, respectively. When both E_α and E_β are 20 mm, a different electrical output is obtained by changing the length of the dielectric film. When both D_α and D_β are 40 mm, 80 mm, and 120 mm, the peak voltages are 880 V, 515 V, and 336 V, respectively (Figure 3(c)), and the peak currents are 238 mA, 166 mA, and 106 mA, respectively (Figure 3(d)). This result indicates that the electric output decreases by increasing the area of the intermediate layer. As the charges in the flow ring are induced by the charges on the PTFE surface, the larger nylon film can decrease the induced charges in the flow ring. Moreover, as shown in Figures 3(e) and 3(f), the electric output decreases on increasing the tangential length of both the electrode and dielectric film. Figures 3(e) and 3(f) show the measured V_{OC} and I_{CC} values when E_β and D_β are 20 mm and 40 mm, respectively. When E_α is 20 mm, 60 mm, 100 mm, and 140 mm and D_α is 40 mm, 80 mm, 120 mm, and 160 mm, respectively, the peak voltage is 870 V, 890 V, 650 V, and 348 V, and the peak current is 236 mA, 244 mA, 152 mA, and 111.2 mA, respectively. This result indicates that the electrical output decreased on increasing the tangential length of the intermediate layer and electrodes. As the main mechanism of FR-TENG is based on the high electrical potential difference between the flow ring and the electrode, the electrical potential of the electrode can be dispersed by the long tangential length. Through this effect, the peak voltage and current can be decreased by increasing the tangential length. In addition, the results of FR-TENGs with different dielectric films and electrode numbers are shown in Supplementary Information 3-5. When different dielectric films and electrode numbers are used, as shown in Supplementary Information 3, V_{OC} and I_{CC} decrease. When the 2, 3, and 4 electrodes and dielectric films are used, the peak V_{OC} is 408 V, 376 V, and 280 V (Supplementary Information 4), and the peak I_{CC} is 100.8 mA, 108.8 mA, and 59.2 mA, respectively (Supplementary Information 5). Although the frequency of the peak output increases on increasing the number of dielectric films and electrodes, the distance between the electrodes decreases. Thus, the peak voltage and current both decrease. Consequently, the FR-TENG with two 20 mm E_α and E_β and 40 mm D_α and D_β of dielectric film and electrode generated the highest peak V_{OC} and I_{CC}.

For practical applications, wearable sleeve-type FR-TENG is fabricated as shown in Figure 4(a). As the nylon-based FR-TENG can also generate a high output, the wearable sleeve-type FR-TENG is fabricated using a commercial nylon-based sleeve. As shown in Figure 4(a), the PTFE film and electrodes are attached to the commercial nylon-based sleeve. As the 20 mm E_α and E_β and 40 mm D_α and D_β of the dielectric film and electrode are most optimal for FR-TENG, the same length of the PTFE films and electrodes is attached to the commercial sleeve. As shown in Figure 4(a), the arm movement allows the flow ring to flow through the arm on the sleeve-type FR-TENG, thus generating a high electrical output. The V_{OC} and I_{CC} of the sleeve-type FR-TENG are shown in Figures 4(b) and 4(c), respectively. The peak V_{OC} and I_{CC} of the sleeve-type FR-TENG resulting from the arm movement are 620 V and 166.4 mA, respectively. In addition, as rectified output is required to power the existing electronics, the rectifying circuit for FR-TENG is constructed as shown in Figure 4(d). As the FR-TENG can generate an electrical output by the electrostatic discharge, an ultrafast switching diode is utilized for the rectifying circuit. The rectified V_{OC} and I_{CC} of sleeve-type FR-TENG are shown in Supplementary Information 6 and 7. Using this electrical output, the sleeve-type FR-TENG can turn on 200 LEDs, as shown in Figure 4(e) and Supplementary Video 1. This result demonstrates that FR-TENG can be used as a power source for electronic devices.

4. Conclusion

In this study, we developed a flow ring-based TENG that can generate high output. The induced charges in the flow ring and the attached electrodes through the opposite charging intermediate layer resulted in a high potential difference between the flow ring and the attached electrode. Thus, the FR-TENG generated high output owing to the electrostatic discharge; peak voltage and current outputs of up to 1020 V and 260 mA, respectively, were obtained. To clarify the effect of the opposite charging intermediate layer, we simulated the electrical field of FR-TENG with and without the opposite charging intermediate layer though the finite element simulation program. By the simulation result, the electric field intensity of FR-TENG with intermediate layer is measured up to 7.33 kV/mm which can generate high output by the electrostatic discharge. Moreover, the electrical outputs of FR-TENG with different areas of the dielectric film and different horizontal lengths are studied to optimize the structure of FR-TENG. By these results, sleeve-type FR-TENG that generated high electrical output with arm movement was fabricated for the practical application. The sleeve-type FR-TENG generated peak voltage and current outputs of up to 620 V and 166.4 mA, respectively. Moreover, 200 LEDs could be turned on with the rectified output of the sleeve-type FR-TENG. We believe that FR-TENG can be used as a power source for wearable devices owing to its high output with human movement.

Data Availability

Data in supplementary information files.

Conflicts of Interest

The authors declare no competing financial interest.

Authors' Contributions

Seh-Hoon Chung was responsible for the conceptualization, methodology, formal analysis, investigation, and visualization and wrote the original draft. Yu Ha Jang was responsible for the conceptualization, methodology, formal analysis, investigation, and visualization and wrote the original draft. Dongchang Kim was responsible for the formal analysis, investigation, and visualization. Joon-seok Lee was responsible for the formal analysis, investigation, and visualization.

Sunghan Kim was responsible for the formal analysis and visualization. Joong Yull Park was responsible for the formal analysis and investigation. Jinkee Hong was responsible for the conceptualization, methodology, supervision, and project administration and wrote and reviewed the manuscript. Sangmin Lee was responsible for the conceptualization, methodology, supervision, and project administration and wrote and reviewed the manuscript. Seh-Hoon Chung and Yu Ha Jang contributed equally to this work.

Acknowledgments

This research was supported by the Chung-Ang University Research Scholarship Grants in 2021 and the National Research Foundation of Korea (NRF) grant funded by the Korea government (MSIT) (No. 2021R1A4A3030268).

Supplementary Materials

The supplementary information file includes supplementary schematics and raw research data. *(Supplementary Materials)*

References

[1] W. Seung, M. K. Gupta, K. Y. Lee et al., "Nanopatterned textile-based wearable triboelectric nanogenerator," *ACS Nano*, vol. 9, no. 4, pp. 3501–3509, 2015.

[2] P. Bai, G. Zhu, Z. H. Lin et al., "Integrated multilayered triboelectric nanogenerator for harvesting biomechanical energy from human motions," *ACS Nano*, vol. 7, no. 4, pp. 3713–3719, 2013.

[3] D. Kim, J. Chung, D. Heo et al., "AC/DC convertible pillar-type triboelectric nanogenerator with output current amplified by the design of the moving electrode," *Advanced Energy Materials*, vol. 12, no. 9, p. 2103571, 2022.

[4] Y. Yang, G. Zhu, H. Zhang et al., "Triboelectric nanogenerator for harvesting wind energy and as self-powered wind vector sensor system," *ACS Nano*, vol. 7, no. 10, pp. 9461–9468, 2013.

[5] J. Wang, W. Ding, L. Pan et al., "Self-powered wind sensor system for detecting wind speed and direction based on a triboelectric nanogenerator," *ACS Nano*, vol. 12, no. 4, pp. 3954–3963, 2018.

[6] B. Chen, Y. Yang, and Z. L. Wang, "Scavenging wind energy by triboelectric nanogenerators," *Advanced Energy Materials*, vol. 8, no. 10, p. 1702649, 2018.

[7] T. Jiang, L. M. Zhang, X. Chen et al., "Structural optimization of triboelectric nanogenerator for harvesting water wave energy," *ACS Nano*, vol. 9, no. 12, pp. 12562–12572, 2015.

[8] C. Zhang, L. Zhou, P. Cheng et al., "Bifilar-pendulum-assisted multilayer-structured triboelectric nanogenerators for wave energy harvesting," *Advanced Energy Materials*, vol. 11, no. 12, p. 2003616, 2021.

[9] L. Xu, T. Jiang, P. Lin et al., "Coupled triboelectric nanogenerator networks for efficient water wave energy harvesting," *ACS Nano*, vol. 12, no. 2, pp. 1849–1858, 2018.

[10] S.-H. Chung, J. Chung, B. Kim, S. Kim, and S. Lee, "Screw pump-type water triboelectric nanogenerator for active water flow control," *Advanced Engineering Materials*, vol. 23, no. 1, p. 2000758, 2021.

[11] J. Luo and Z. L. Wang, "Recent progress of triboelectric nanogenerators: from fundamental theory to practical applications," *EcoMat*, vol. 2, no. 4, article e12059, 2020.

[12] M. Song, J. Chung, S. H. Chung et al., "Semisolid-lubricant-based ball-bearing triboelectric nanogenerator for current amplification, enhanced mechanical lifespan, and thermal stabilization," *Nano Energy*, vol. 93, article 106816, 2022.

[13] D. Bhatia, S. H. Jo, Y. Ryu, Y. Kim, D. H. Kim, and H. S. Park, "Wearable triboelectric nanogenerator based exercise system for upper limb rehabilitation post neurological injuries," *Nano Energy*, vol. 80, article 105508, 2021.

[14] K. N. Kim, J. Chun, J. W. Kim et al., "Highly stretchable 2D fabrics for wearable triboelectric nanogenerator under harsh environments," *ACS Nano*, vol. 9, no. 6, pp. 6394–6400, 2015.

[15] K. Cha, J. Chung, D. Heo et al., "Lightweight mobile stick-type water-based triboelectric nanogenerator with amplified current for portable safety devices," *Science and Technology of Advanced Materials*, vol. 23, no. 1, pp. 161–168, 2022.

[16] C. Ning, L. Tian, X. Zhao et al., "Washable textile-structured single-electrode triboelectric nanogenerator for self-powered wearable electronics," *Journal of Materials Chemistry A*, vol. 6, no. 39, pp. 19143–19150, 2018.

[17] T. Zhou, C. Zhang, C. B. Han, F. R. Fan, W. Tang, and Z. L. Wang, "Woven structured triboelectric nanogenerator for wearable devices," *ACS Applied Materials & Interfaces*, vol. 6, no. 16, pp. 14695–14701, 2014.

[18] J.-N. Kim, J. Lee, T. W. Go et al., "Skin-attachable and biofriendly chitosan-diatom triboelectric nanogenerator," *Nano Energy*, vol. 75, article 104904, 2020.

[19] L. Wang and W. A. Daoud, "Highly flexible and transparent polyionic-skin triboelectric nanogenerator for biomechanical motion harvesting," *Advanced Energy Materials*, vol. 9, no. 5, p. 1803183, 2018.

[20] S. Li, J. Wang, W. Peng et al., "Sustainable energy source for wearable electronics based on multilayer elastomeric triboelectric nanogenerators," *Advanced Energy Materials*, vol. 7, no. 13, p. 1602832, 2017.

[21] S. Yan, Z. Zhang, X. Shi et al., "Eggshell membrane and expanded polytetrafluoroethylene piezoelectric-enhanced triboelectric bio-nanogenerators for energy harvesting," *International Journal of Energy Research*, vol. 45, no. 7, pp. 11053–11064, 2021.

[22] W. Liu, Z. Wang, G. Wang et al., "Integrated charge excitation triboelectric nanogenerator," *Nature Communications*, vol. 10, no. 1, pp. 1–9, 2019.

[23] J. Chung, S. H. Chung, Z. H. Lin, Y. Jin, J. Hong, and S. Lee, "Dielectric liquid-based self-operating switch triboelectric nanogenerator for current amplification via regulating air breakdown," *Nano Energy*, vol. 88, article 106292, 2021.

[24] D. Hong, Y. M. Choi, Y. Jang, and J. Jeong, "A multilayer thin-film screen-printed triboelectric nanogenerator," *International Journal of Energy Research*, vol. 42, no. 11, pp. 3688–3695, 2018.

[25] X. Cui, Y. Zhang, G. Hu, L. Zhang, and Y. Zhang, "Dynamical charge transfer model for high surface charge density triboelectric nanogenerators," *Nano Energy*, vol. 70, article 104513, 2020.

[26] J. Jeong, B. Yoo, E. Jang, I. Choi, and J. Lee, "Metal electrode polarization in triboelectric nanogenerator probed by surface charge neutralization," *Nanoscale Research Letters*, vol. 17, no. 1, pp. 1–9, 2022.